Destructiveness of Earthquake Ground Motions: "Intensity Measures" versus Sliding Displacement

Ev. Garini & G. Gazetas
Soil Mechanics Laboratory, National Technical University, Athens, Greece

ABSTRACT: The scope is to estimate qualitatively and quantitatively the potential destructiveness of earthquakes on structures characterized by inelastic response. To this end, earthquake records are utilized studying several seismological parameters as destructiveness indices of earthquake shaking. We employ twenty six widely acknowledged indices, such as the Arias intensity, the Housner intensity, the destructiveness potential factor, the acceleration spectrum intensity, the specific energy density etc. A large number (eighty nine) of earthquake records are selected, paying particular attention to include ground motions with strong near-fault characteristics: forward directivity and fling. Apart from the seismological parameters, sliding displacement on an inclined plane is utilized as an additional destructiveness index representative of the inelastic response of structural systems. In particular, we adopt the Newmark's model of a rigid block resting on an inclined surface (governed by the Coulomb friction law) subjected to seismic excitation. The results are presented in form of sliding displacement versus each one of the seismic indexes. By comparison we conclude to specific indices which can describe satisfactorily the inelastic response.

1 INTRODUCTION–SCOPE OF STUDY

For systems whose deformation involves restoring mechanisms with a dominant linear component, the viscous-elastic response spectra, S_A S_V S_D, of a particular accelerogram provide an efficient indication of its potential to cause unacceptable amplitudes of deformation in various structures (as a function of their elastic fundamental period). However, for systems with strongly nonlinear and/or inelastic restoring mechanisms, elastic response spectra are often inadequate descriptors of the damage potential. This is absolutely true in cases where no elastic component of restoring mechanism is present, such as with systems which rely solely on friction for lateral support. An example in structural engineering is the (flat) friction–isolated structures. In geotechnical engineering, gravity retaining walls and slopes rely primarily on frictional interfaces (rather than elasticity) for lateral seismic support. In general, ductile structures designed to respond mainly in the inelastic region, have restoring force-displacement relationships which resemble the frictional mechanism.

An abstraction has been inspired by the above applications. To assess the potential of an accelerogram to inflict large irrecoverable deformation on highly inelastic systems, the seismic behavior of two idealized systems is explored. They are to be thought of as analogues of actual inelastic systems: (a) the sliding of a rigid block on a horizontal base, and (b) sliding of a rigid block on an inclined ($\geq 25^o$) base, [called Newmark's sliding in the geotechnical literature]. These two systems are characterized by a rigid–plastic symmetric (a), or asymmetric (b), restoring–force–displacement relationships obeying Coulomb's friction law, as presented in Figure 1. The supporting base of each system is subjected to a particular ground motion under investigation, and the size of the resulting inelastic/nonlinear response serves as an index of the damage

that this motion can inflict on the corresponding class of inelastic systems—the "destructiveness" potential of the motion.

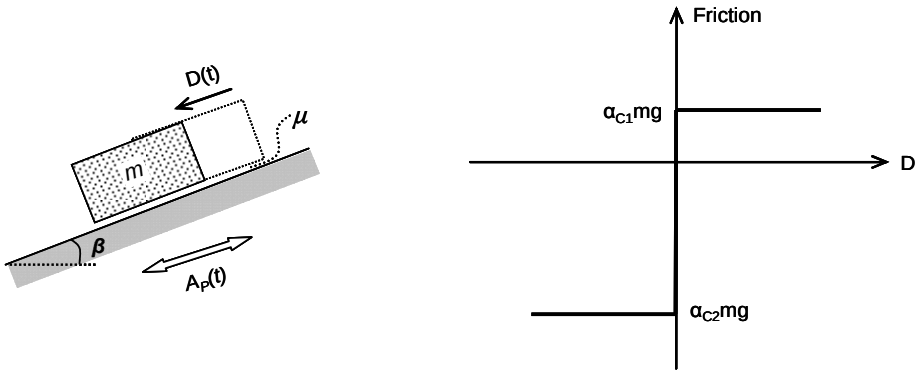

Figure 1. Schematic representation of the Newmark 1965 sliding-block analogue and friction force as a function of slip displacement.

2 TYPES OF DESTRUCTIVENESS INDICES

2.1 *Newmark's asymmetric sliding response*

The analysis of the behavior of a block on horizontal or inclined base which is subjected to motion A(t) parallel to the plane is obtained from elementary rigid body kinematics along with Newton's second law of motion. The critical acceleration(s) which must be exceeded for slippage to be initiated are simply:

$$A_{C1} = (\mu \cos\beta - \sin\beta)\, g \quad (1)$$

$$A_{C2} = (\mu \cos\beta + \sin\beta)\, g \quad (2)$$

in which A_C = the critical acceleration for sliding in either direction of the symmetric system; μ = the (constant) coefficient of friction; A_{C1} and A_{C2} are the critical accelerations for downhill and uphill sliding respectively, for the asymmetric system of a plane inclined at an angle β. Usually $A_{C1} << A_{C2}$ and as a result sliding takes place only downhill.

Whenever the base acceleration exceeds A_C or A_{C1} (or, rarely, A_{C2}) slippage of the block takes place with respect to the base. This slippage lasts only momentarily, thanks to the transient nature of earthquake shaking; it terminates as soon as the velocities of the base and the block equalize. And the process continues until the motions of both the block and the base eventually terminate. The maximum and/or the permanent amount of slippage is taken as the damage of the idealized system (analogue).

2.2 *Intensity indices*

Numerous parameters of a ground motion have been proposed over the years to serve as indices of the "damage potential" of a ground motion. Such indices are often called "Intensity Measures" (IM). Several such IM are tested herein against the amount of slippage induced by a ground motion. Specifically, the examined indices include: the Arias intensity (I_A), the Housner intensity (I_H), the RMS acceleration; or velocity; or displacement (A_{RMS}, V_{RMS}, D_{RMS}), the characteristic intensity (I_C), the specific energy density (S_E), the cumulative absolute velocity (CAV), the sustained maximum acceleration and velocity (SMA and SMV respectively), acceleration and velocity spectrum intensity (ASI and VSI), the acceleration parameter A_{95}, the predominant period (T_P), the mean period (T_{mean}), the significant duration (D_{sig}), the destructiveness potential factor (P_D), and the ratio V_{max}^2/A_{max} of the peak velocity squared divided by PGA. Next all these parameters are presented in detail:

- Arias Intensity, I_A, is proportional to the integral of the squared ground acceleration A(t) time history:

$$I_A = \frac{\pi}{2g}\int A^2(t)dt \tag{3}$$

- Housner Intensity, I_H, is the integral of the pseudo-velocity spectrum over the period range [0.1 s, 2.5 s] :

$$I_H = \int_{0.1}^{2.5} S_V(T, \xi = 5\%)dT \tag{4}$$

where $S_V(T,\xi)$ is the pseudo-velocity response spectrum (Housner, 1952).

- RMS acceleration, A_{RMS}, is the square root of the mean acceleration:

$$A_{RMS} = \sqrt{\frac{\int A^2(t)dt}{T_D}} \tag{5}$$

where T_D is the length of the record and A(t) is the acceleration time history.

- RMS velocity, V_{RMS}, is the root mean square of velocity:

$$V_{RMS} = \sqrt{\frac{\int V^2(t)dt}{T_D}} \tag{6}$$

where T_D is the length of the record and V(t) is the velocity time history.

- RMS displacement, D_{RMS}, is the root mean square of displacement:

$$D_{RMS} = \sqrt{\frac{\int D^2(t)dt}{T_D}} \tag{7}$$

where T_D is the length of the record and D(t) is the displacement time history.

- Characteristic Intensity, I_C, is defined as:

$$I_C = (A_{RMS})^{3/2}\sqrt{T_D} \tag{8}$$

where T_D is the length of the record.

- Specific Energy Density, S_E, is calculated from the expression:

$$S_E = \frac{\beta_S \rho_S}{4}\int V^2(t)dt \tag{9}$$

where V(t) is the ground velocity time history, β_S is the wave velocity and ρ_S is the mass density of the recording site (Sarma, 1971).

- Cumulative Absolute Velocity, CAV, is defines as:

$$CAV = \sum_{i=1}^{N} H(PGA_i - A_{\min})\int_{t_i}^{t_{i+1}} |A(t)|dt \tag{10}$$

where A(t) is the ground acceleration, N is the number of 1-second time windows in the time series, PGA_i is the PGA (in g) during time window i, t_i is the start time of time window i, A_{min} is an acceleration threshold (user-defined, but usually taken as 0.025g) to exclude low amplitude motions contributing to the sum, and H(x) is the Heaviside step function (unity for x>0, zero otherwise).

- Sustained Maximum Acceleration, SMA, is the third highest absolute peak in the acceleration time history, proposed by Nuttli (1979).

- Sustained Maximum Velocity, SMV, is the third highest absolute peak in the velocity time history, proposed by Nuttli (1979).

- Acceleration Spectrum Intensity, ASI, is calculated as:

$$ASI = \int S_A(5\%, T)dT \tag{11}$$

where $S_A(5\%,T)$ is the spectral acceleration for 5% damping and T is natural period [see Kramer (1996)].

- Velocity Spectrum Intensity, VSI, is calculated from:

$$VSI = \int S_V(5\%, T)dT \tag{12}$$

where $S_V(5\%,T)$ is the spectral pseudo-velocity for 5% damping and T is natural period [see Kramer (1996)].

- Acceleration parameter A_{95} is the level of acceleration which contains up to 95% of the Arias Intensity [Sarma & Yang (1987)].

- Predominant Period, T_P, evaluated using the 5% damped acceleration response spectrum, and corresponds to the period of the maximum spectral acceleration, as long as $T_P > 0.20$ sec.

- Mean Period, T_{mean}, is defined based on the Fourier amplitude spectrum. The mathematical expression is:

$$T_{mean} = \frac{\sum\left(\frac{C_i^2}{f_i}\right)}{\sum C_i^2} \tag{13}$$

where C_i is the Fourier amplitude for each frequency f_i within the range 0.25–20 Hz.

- Significant Duration, D_{signif}, is the interval of time between the accumulation of 5% and 95% of Arias Intensity.

- Destructiveness Potential Factor, P_D, is the ratio between the Arias Intensity I_A and the square of the number of zero crossings per second of the accelerogram ν_0^2:

$$P_D = \frac{I_A}{\nu_O^2} = \frac{\pi}{2g}\frac{\int A^2(t)dt}{\nu_O^2} \tag{14}$$

as introduced by Araya & Saragoni (1984) and by Crespellani et all (2003).

3 GROUND MOTIONS

A large number (99) of recorded ground motions are utilized for this test. The selection was such as to cover many of the well known accelerograms from earthquakes of the last 30 years, and to include motions bearing near-fault characteristics: directivity and fling effects. Table 1

lists these records along with their PGA, PGV, and PGD values. Each accelerogram imposed with its recorded sign (normal polarity) and with opposite sign (reverse polarity).

Table 1. List of significant earthquake records bearing the effects of ‘directivity’ and ‘fling’, utilized as excitations in this study.

Record Name	PGA [g]	PGV [m/s]	PGD [m]
Fukiai	0.763	1.232	0.134
JMA–0º	0.830	0.810	0.177
JMA–90º	0.599	0.761	0.199
Nishi Akashi–0º	0.509	0.357	0.091
Nishi Akashi–90º	0.503	0.356	0.109
Shin Kobe–NS	0.422	0.688	0.169
Takarazuka–0º	0.693	0.682	0.274
Takarazuka–90º	0.694	0.853	0.167
Takatori–0º	0.611	1.272	0.358
Takatori–90º	0.616	1.207	0.328
No 4–140º	0.485	0.374	0.202
No 4–230º	0.360	0.766	0.590
No 5–140º	0.519	0.469	0.353
No 5–230º	0.379	0.905	0.630
No 6–140º	0.410	0.649	0.276
No 6–230º	0.439	1.098	0.658
No 7–140º	0.338	0.476	0.246
No 7–230º	0.463	1.093	0.447
No 9 Differential Array–270º	0.352	0.712	0.458
No 9 Differential Array–360º	0.480	0.408	0.140
Lucerne–0º	0.785	0.319	0.164
Lucerne–275º	0.721	0.976	0.703
Joshua Tree–0º	0.274	0.275	0.098
Joshua Tree–90º	0.284	0.432	0.145
Pacoima Dam–164º	1.226	1.124	0.361
Pacoima Dam–254°	1.160	0.536	0.111
Erzincan (Station 95)–EW	0.496	0.643	0.236
Erzincan (Station 95)–NS	0.515	0.839	0.312
Los Gatos Presentation Center–0º	0.563	0.948	0.411
Los Gatos Presentation Center–90º	0.605	0.510	0.115
Saratoga Aloha Avenue–0º	0.512	0.412	0.162
Saratoga Aloha Avenue–90°	0.324	0.426	0.275
Karakyr–0º	0.608	0.654	0.253
Karakyr–90º	0.718	0.716	0.237
Jensen Filtration Plant–22º	0.424	0.873	0.265
Jensen Filtration Plant–292º	0.592	1.201	0.249
L.A. Dam–64º	0.511	0.637	0.211
L.A. Dam–334º	0.348	0.508	0.151
Newhall Firestation–90º	0.583	0.524	0.126
Newhall Firestation–360º	0.589	0.753	0.182
Pacoima Dam (downstream)–175º	0.415	0.456	0.050
Pacoima Dam (downstream)–265º	0.434	0.313	0.048
Pacoima Kagel Canyon–90°	0.301	0.379	0.095
Pacoima Kagel Canyon–360°	0.432	0.452	0.069
Rinaldi–228°	0.837	1.485	0.261
Rinaldi–318°	0.472	0.627	0.166
Santa Monica City Hall–90°	0.883	0.403	0.102
Santa Monica City Hall–360°	0.369	0.232	0.059
Sepulveda VA–270°	0.753	0.848	0.186
Sepulveda VA–360°	0.939	0.766	0.149

Simi Valley Katherine Rd–0º	0.877	0.409	0.053
Simi Valley Katherine Rd–90°	0.640	0.378	0.051
Sylmar Hospital–90º	0.604	0.744	0.165
Sylmar Hospital–360º	0.843	1.027	0.256
TCU 052–EW	0.350	1.743	4.659
TCU 052–NS	0.437	2.186	7.319
TCU 065–EW	0.450	1.298	1.820
TCU 065–NS	0.554	0.876	1.254
TCU 067–EW	0.487	0.973	1.953
TCU 067–NS	0.311	0.536	0.849
TCU 068–EW	0.491	2.733	7.149
TCU 068–NS	0.353	2.892	8.911
TCU 075–EW	0.324	1.143	1.692
TCU 075–NS	0.254	0.360	0.414
TCU 076–EW	0.335	0.706	1.223
TCU 076–NS	0.416	0.617	0.662
TCU 080–EW	0.968	1.076	0.186
TCU 080–NS	0.902	1.025	0.340
TCU 084–EW	0.986	0.923	0.910
TCU 084–NS	0.419	0.486	0.966
TCU 102–EW	0.297	0.870	1.478
TCU 102–NS	0.168	0.705	1.062
Duzce–180º	0.312	0.474	0.285
Duzce–270º	0.358	0.464	0.176
Sakarya–EW	0.330	0.814	2.110
Yarimca–60º	0.231	0.906	1.981
Yarimca–330º	0.322	0.867	1.493
Tabas–LN	0.836	0.978	0.387
Tabas–TR	0.852	1.212	0.951
National Geographical Institute–180º	0.392	0.566	0.206
National Geographical Institute–270º	0.524	0.753	0.116
Geotechnical Investigation Center–90º	0.681	0.793	0.119
Geotechnical Investigation Center–180º	0.412	0.602	0.201
Institute of Urban Construction–90º	0.380	0.441	0.173
Institute of Urban Construction–180º	0.668	0.595	0.112
Bolu–0º	0.728	0.564	0.231
Bolu–90º	0.822	0.621	0.135
Duzce–180º	0.348	0.600	0.421
Duzce–270º	0.535	0.835	0.516

4 ANALYSES RESULTS

At this point, the results here are for the asymmetric sliding system, as shown in Figure 1. Figure 2 illustrates the correlation between Arias intensity and slippage. Figure 3 demonstrates slippage, D, according to the peak acceleration, velocity and displacement values for all the 99 ground motions. Next, at Figure 4 sliding response is depicted in correlation with the potential destructiveness factor, P_D.

Figures 5-9 pictured asymmetric sliding versus the rest Intensity Measures (IM). Furthermore, Table 2 presents the correlation index, R^2, between asymmetric sliding response, D, and each IM, covering the parametric range of our study.

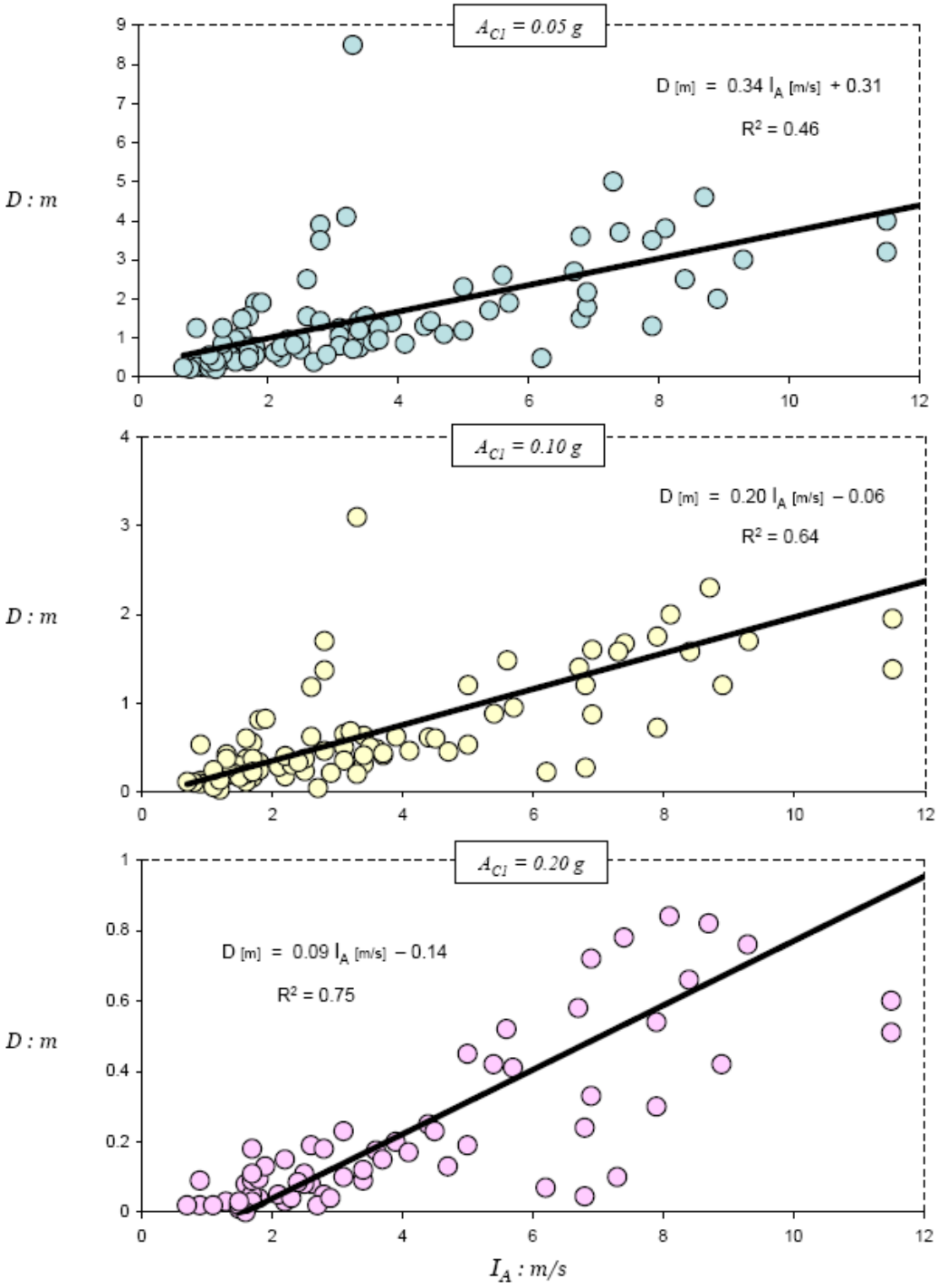

Figure 2. Correlation between the Arias Intensity, I_A, of the records utilized as excitation in our study and the triggered sliding displacement, D, for three values of critical acceleration A_C. A linear trend line is plotted for each case, with the correlation index, R^2, stated.

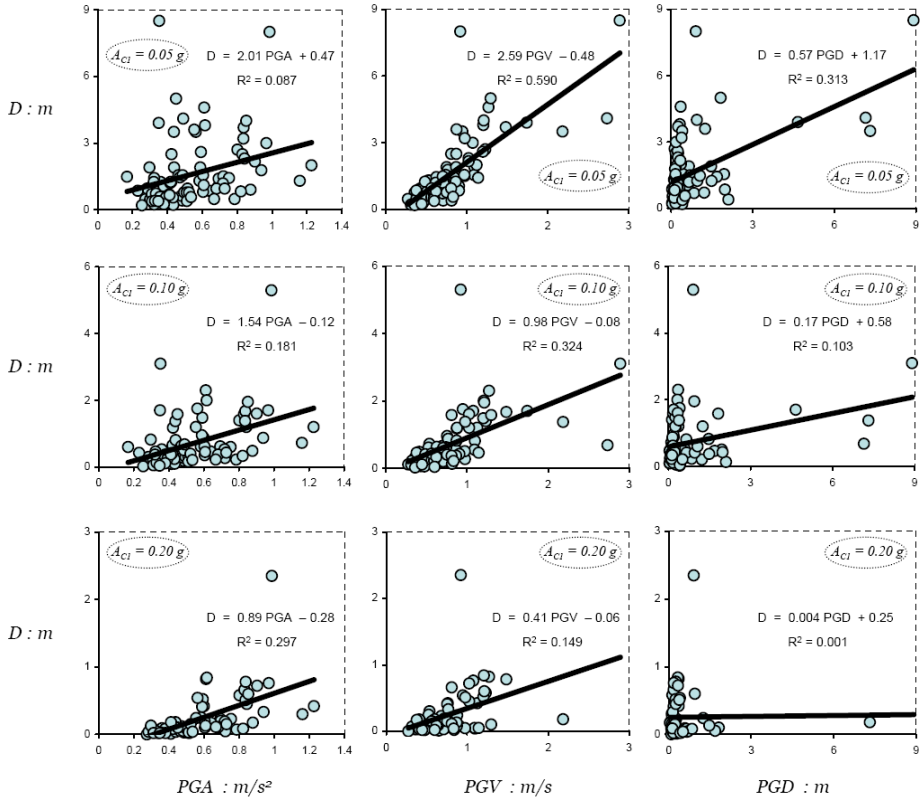

Figure 3. Slippage, D, with respect to the most widely used ground motion characteristics: (a) peak ground acceleration–in the first column from the left, (b) peak ground velocity–in the second column, and (c) peak ground displacement–in the last column to the left.

Table 2. Correlation index, R, between asymmetric sliding response, D, and seismic indices of destructiveness, covering the parametric range of our study.

Correlation Index, R	A_{C1} = 0.05g	A_{C1} = 0.10g	A_{C1} = 0.20g
Peak Ground Acceleration, PGA	0.09	0.18	0.29
Peak Ground Velocity, PGV	0.59	0.32	0.15
Peak Ground Displacement, PGD	0.31	0.10	0.001
Arias Intensity, I_A	0.46	0.64	0.75
Destructiveness Potential Factor, P_D	0.58	0.73	0.69
Housner Intensity, I_H	0.52	0.67	0.71
RMS Acceleration, A_{RMS}	0.23	0.25	0.24
RMS Velocity, V_{RMS}	0.54	0.26	0.12
RMS Displacement, D_{RMS}	0.07	0.03	0.004
Spectral Displacement at T=1 sec, $S_{D/(T=1s)}$	0.36	0.53	0.61
Spectral Displacement at T=2 sec, $S_{D/(T=2s)}$	0.61	0.61	0.45
Spectral Displacement at T=3 sec, $S_{D/(T=3s)}$	0.31	0.19	0.05
Spectral Displacement at T=4 sec, $S_{D/(T=4s)}$	0.23	0.08	0.00
Characteristic Intensity, I_C	0.39	0.51	0.55
Specific Energy Density, S_E	0.49	0.23	0.07
Cumulative Absolute Velocity, CAV	0.44	0.51	0.52
Sustained Maximum Acceleration, SMA	0.16	0.23	0.29
Sustained Maximum Velocity, SMV	0.53	0.36	0.16
Acceleration Spectrum Intensity, ASI	0.08	0.17	0.30
Velocity Spectrum Intensity, VSI	0.53	0.68	0.73
Acceleration Parameter, A_{95}	0.11	0.19	0.27
Predominant Period, T_P	0.17	0.15	0.14
Mean Period, T_{mean}	0.15	0.07	0.002
Significant Duration, D_{sig}	0.001	0.003	0.006

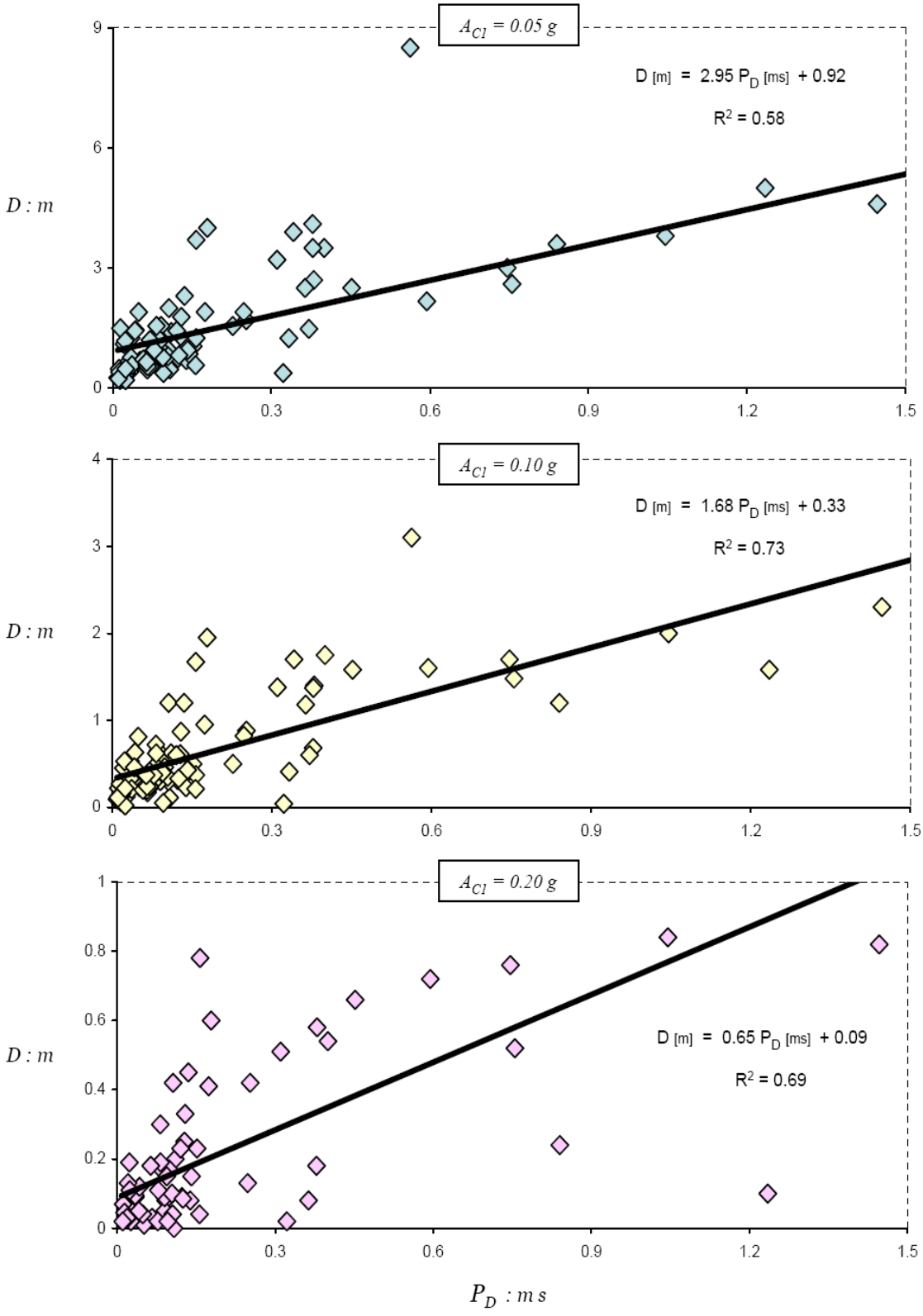

Figure 4. The influence of potential destructiveness factor P_D (as defined by Araya & Saragoni, 1984) on sliding displacement D, for three levels of critical yielding acceleration A_C: 0.05 g, 0,1 g, and 0.2 g.

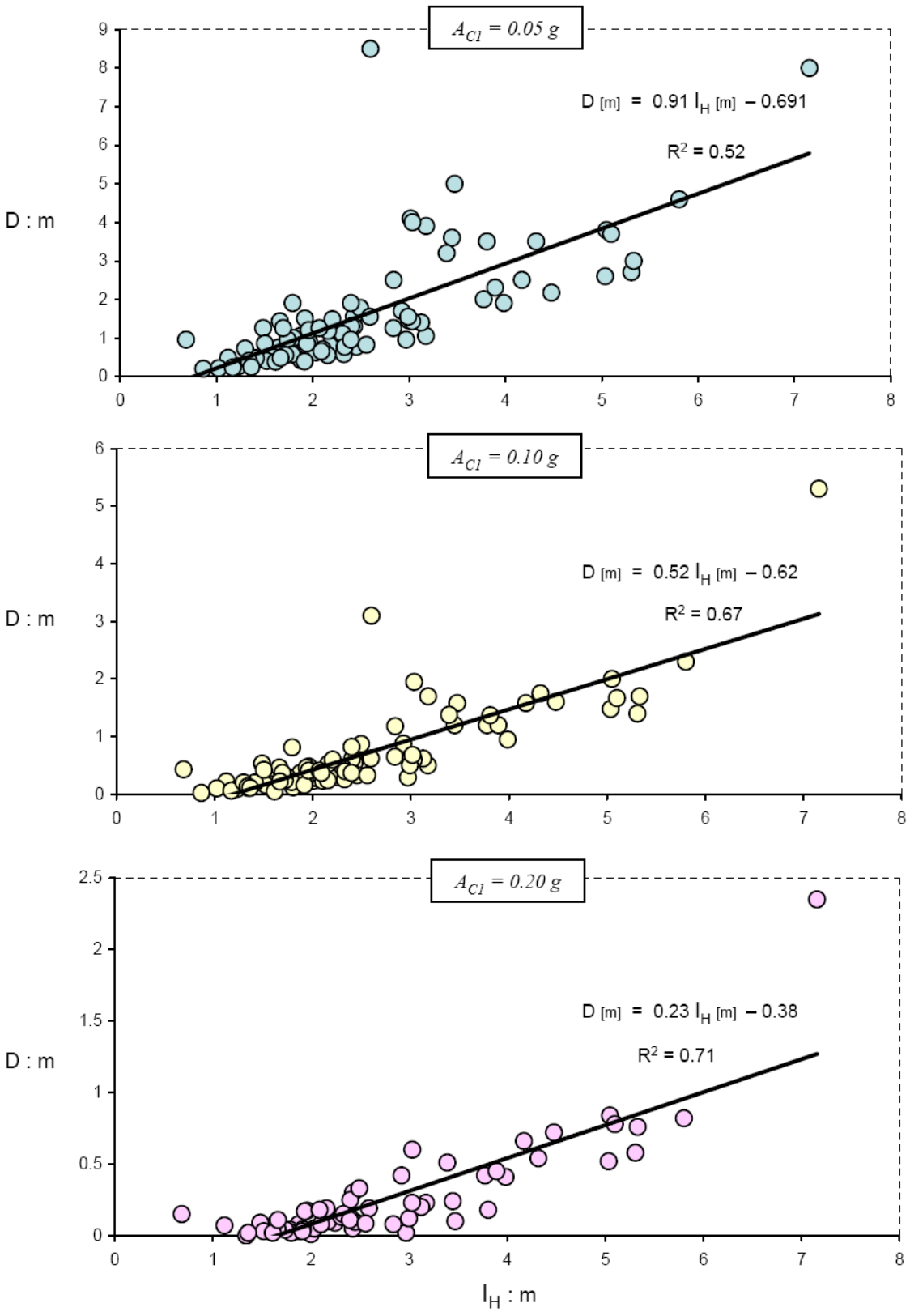

Figure 5. Correlation between the Housner Intensity, I_H, of the records utilized as excitation in our study and the triggered sliding displacement, D, for three values of critical acceleration A_C. A linear trend line is plotted for each case, with the correlation index, R^2, stated.

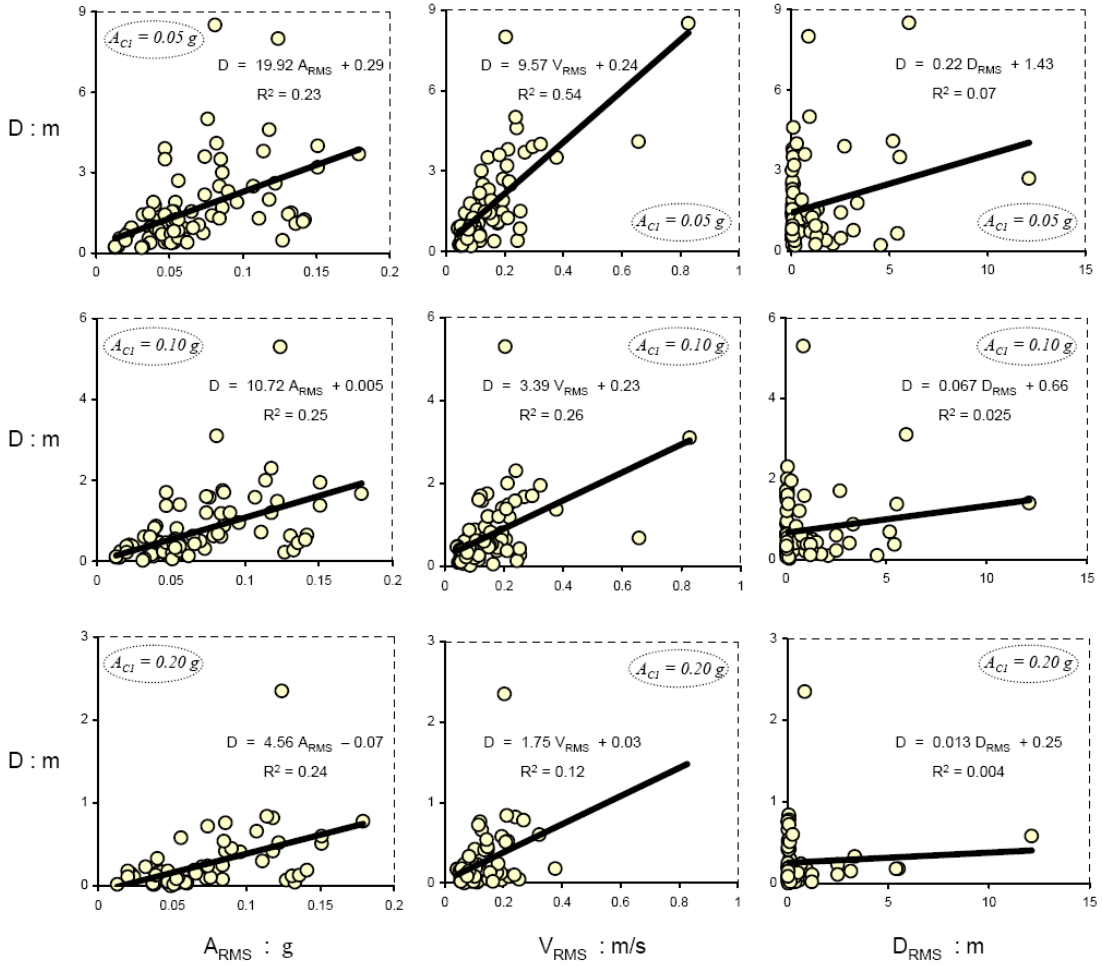

Figure 6. Slippage, D, in connection with the Root Mean Square values: (a) RMS acceleration–in the first column from the left, (b) RMS velocity–in the second column, and (c) RMS displacement–in the last column to the left.

5 CONCLUSIONS

As an index of the structural response of yielding systems we adopt the Newmark's model of a rigid block resting on an inclined plane with Coulomb friction interface subjected to seismic excitation. For the latter, 99 actual accelerograms, many of which bear the effects of near-fault forward directivity or fling step, are utilized unscaled. The resulting sliding displacements are then correlated with 26 widely used "intensity measures" (or "indices of destructiveness potential"), such us the peak ground acceleration, the peak ground velocity, peak ground displacement, the Arias intensity, the Housner intensity, the destructiveness potential factor, the acceleration spectrum intensity, the specific energy density, and others. The conclusions are drawn regarding the performance of each index vis-à-vis the ensemble of sliding displacements, as summarized in Table 2.

For small ratios of A_{C1}, the intensity indices that provide the best correlation with the induced sliding displacement are in descending order: the spectral displacement at period of 2 seconds ($S_{D/(T=2s)}$), the destructiveness potential factor (P_D), and the peak ground velocity (PGV). For large ratios of A_{C1}, best correlations present the Arias intensity (I_A), the Housner intensity (I_H), and the velocity spectrum intensity (VSI).

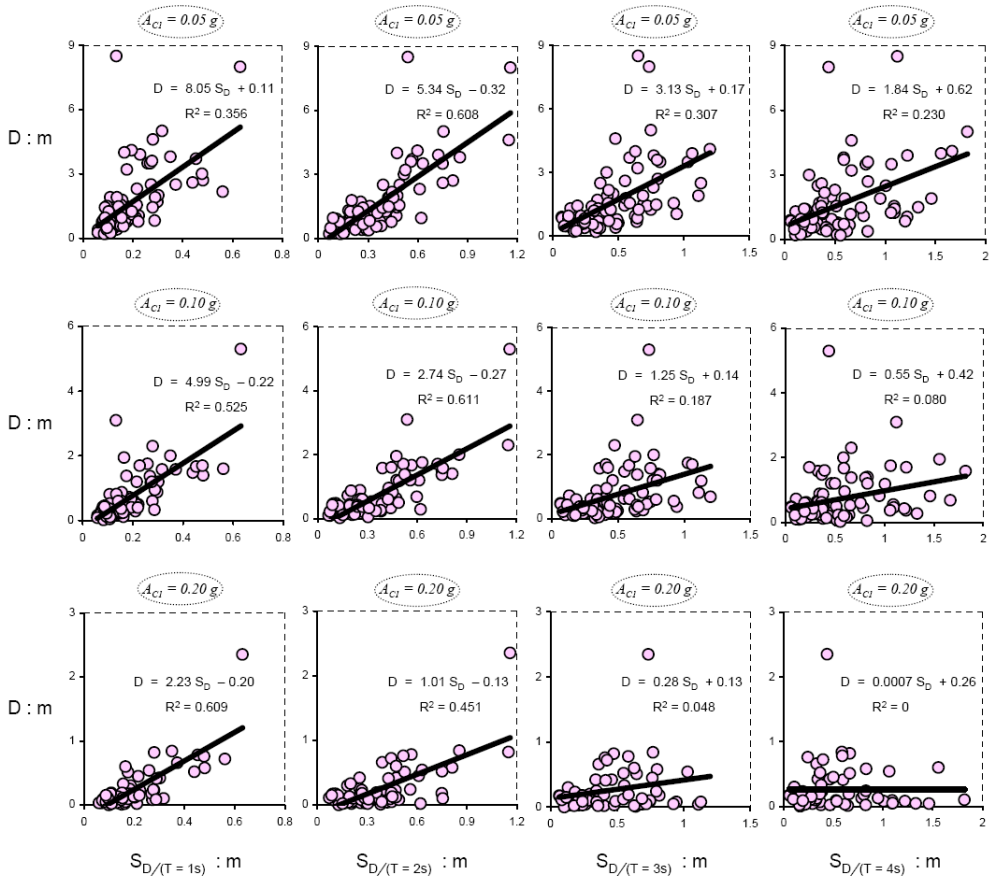

Figure 7. Correlation of slippage, D, with its corresponding spectral displacement at four different periods, T: for period of 1, 2, 3, and 4 seconds.

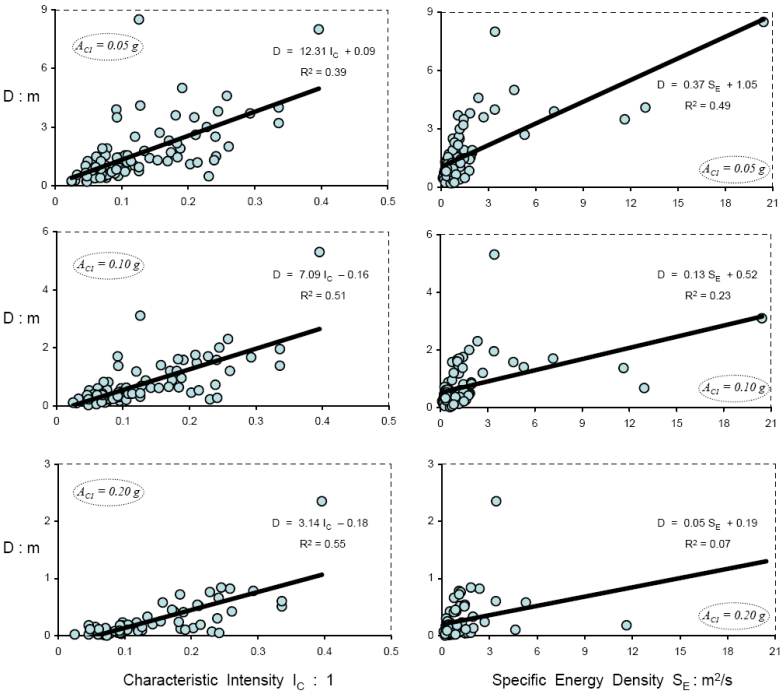

Figure 8. Influence of the dimensionless parameter of characteristic intensity, I_C, on slippage, D, at the left hand-side and effect of specific energy density, S_E, at the right. Observe the poor correlation of the induced slippage with the energy density value of each earthquake event.

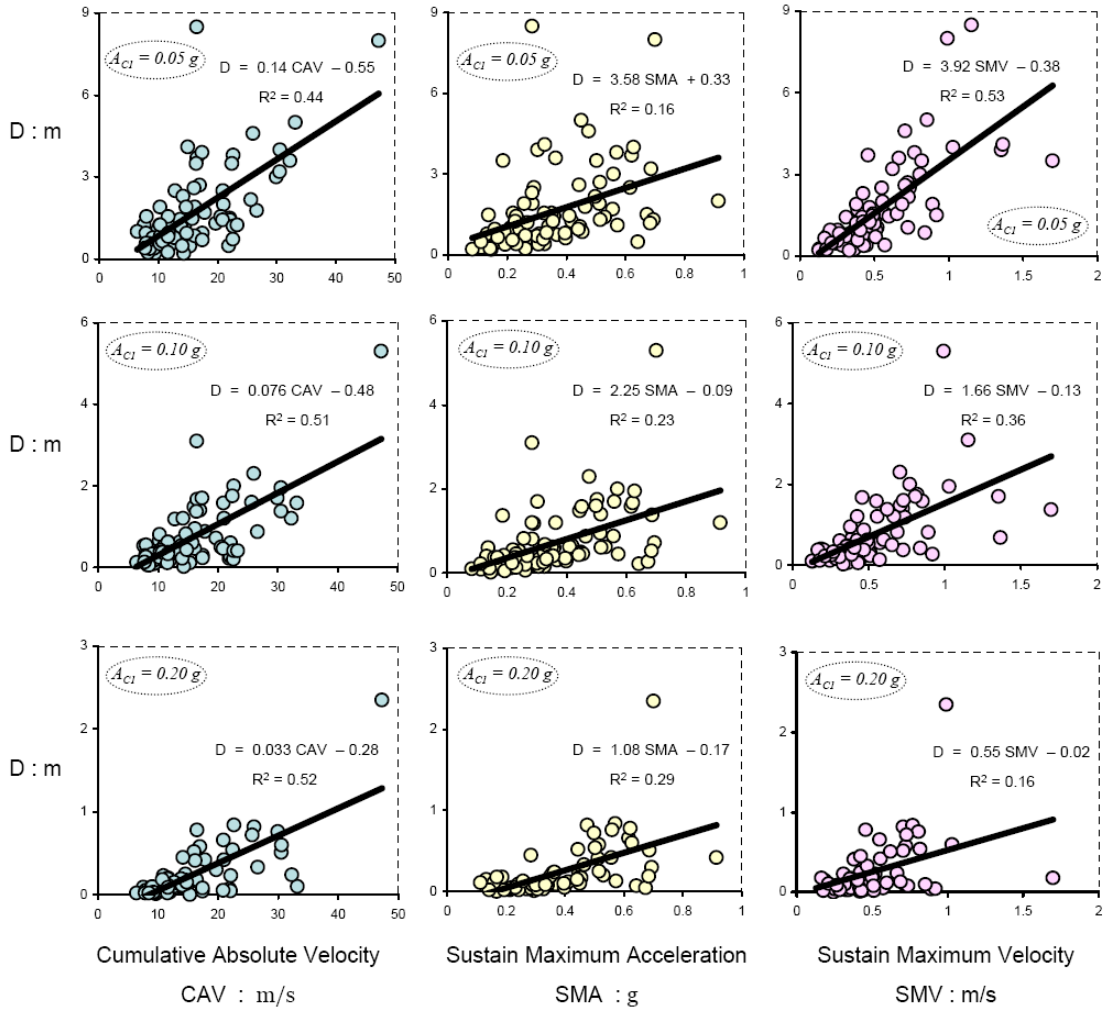

Figure 9. Slippage, D, as a function of : (a) the cumulative absolute velocity–in the first column from the left, (b) the sustained maximum acceleration–in the second column, and (c) the sustained maximum velocity–in the last column to the left.

6 ACKNOWLEDGEMENTS

The financial support for the work outlined in this paper has been provided under the collaborative research project “PERPETUATE”, under contract number ENV.2009.3.2.1.1.

7 REFERENCES

Arias, A. 1970. A measure of earthquake intensity. *Seismic Design for Nuclear Power Plants (ed. R.J. Hansen)*, MIT Press, Cambridge, Massachusetts, 438-483.

Bommer, J. J. & Martinez, P. 1999. The effective duration of earthquake strong motion. *Journal of Earthquake Engineering*, 3(2), 127-172.

Gazetas, G., Garini, E., Anastasopoulos, I. & Georgarakos, T. 2009. Effects of near–fault ground shaking on sliding systems. *J. Geotech. Geoenviron. Engng*, ASCE 135(12), 1906-1921.

Garini, E., Gazetas, G. & Anastasopoulos, I. 2010. Asymmetric ‘Newmark’ sliding caused by motions containing severe ‘directivity’ and ‘fling’ pulses. *Géotechnique*, Vol.60, doi: 10.1680/geot.2010.60.00.1

Hancock, J. & Bommer, J. J. 2005. The effective number of cycles of earthquake ground motion. *Earthquake Engineering & Structural Dynamics*, 34, 637-664.

Newmark, N. M. 1965. Effects of earthquakes on dams and embankments, *Géotechnique* 15(2), 139-160.
PEER Strong Motion Database. 2002. *http://peer.berkeley.edu/smcat/data.html.*
Rathje, E. M., Faraj, F., Russell, S. & Bray, J. D. 2004. Empirical relationships for frequency content parameters of earthquake ground motions. *Earthquake Spectra*, 20(1), 119-144.
Sarma, S. K. & Yang, K. S. 1987. An evaluation of strong motion records and a new parameter A95. *Earthquake Engineering & Structural Dynamics*, 15(1), 119-132.
Housner, G.V. 1952. Spectrum intensities of strong motion earthquakes. *Proceedings of the Symposium on Earthquake and Blast Effects on Structures*, EERI, Oakland California, 20–36.